



# Dust extinction and environmental properties of GRB afterglows

Tayyaba Zafar<sup>1</sup>

Dark Cosmology Centre, Niels Bohr Institute, University of Copenhagen, Juliane Maries Vej 30, DK-2100 Copenhagen Ø, Denmark. e-mail: tayyaba@dark-cosmology.dk

**Abstract.** Long-duration Gamma-ray bursts (GRBs) occur in star-forming regions and have simple synchrotron emission spectra. In a sample study of 41 GRB afterglows 21 require a cooling break between the X-ray and the optical/near-infrared. Excluding one outlier, GRB 080210, the average spectral slope change is  $\Delta\beta = 0.51$  with a standard deviation of 0.02 consistent with the prediction of synchrotron model. To understand environmental properties of GRBs, gas-to-dust ratios are compared with the metallicities of GRB afterglows, indicating an anti-correlation between the two values. This anti-correlation is consistent with the Local Group relation. Since GRBs occur in star-forming regions, it was anticipated that there should be significant dust extinction of GRB optical afterglows. The vast majority of GRB extinction curves are featureless—the 2175 Å bump so far has been detected in the optical spectra of only four GRBs. Using the Fitzpatrick & Massa (1990) extinction model, the strength of the bump is estimated for 38 GRB afterglows, preferring Small Magellanic Cloud (SMC)-type extinction curve, finding in no significant detection of the 2175 Å bump. The comparison of GRB afterglows to the Local Group sightlines suggests that GRB afterglows usually have lower bump strength for a given  $A_V$ .

**Key words.** Galaxies: high-redshift - ISM: dust, extinction - Gamma-ray burst: general

## 1. Introduction

GRBs are transient sources usually followed by their long lasting counterparts, emitting large amount of energy across the full range of the electromagnetic spectrum, called as afterglows. Long-duration bursts are associated with core-collapse supernovae (Woosley 1993; Galama et al. 1998a; Hjorth et al. 2003; Stanek et al. 2003), occur in star-forming regions in star-forming galaxies (Bloom et al. 2002), have simple synchrotron emission spectra ( $F_\nu \propto \nu^{-\beta}$ ; Rees & Mészáros 1992; Sari et al. 1998)

and are observable over a vast range of redshifts ( $z = 0.0086-8.2$ ), reaching further distances than quasars (QSOs).

Dust and gas absorption leave imprint on GRB afterglow spectra. The observations of GRB afterglows probe gas and dust in the interstellar medium (ISM) of young, distant actively star-forming galaxies, as well as the intervening intergalactic medium (IGM) along these lines of sight. The intrinsic Spectral Energy Distribution (SED) of GRB afterglows is a direct approach to study the surrounding environments of GRBs and allows the dust extinction curve to be well modelled.

---

Send offprint requests to: T. Zafar

Extinction curves are the prime diagnostic tool to study dust extinction in the optical and UV energy bands. The extinction curves of the Milky Way (MW), Large Magellanic Cloud (LMC) and SMC are studied in great detail and typically obtained by comparing pairs of stars (Fitzpatrick & Massa 1986; Cardelli et al. 1989; Pei 1992; Gordon et al. 2003; Fitzpatrick & Massa 2007). The method is not applicable outside the Local Group because individual stars are difficult and impossible to observe. GRB afterglows occur in star-forming galaxies at high redshifts and give us a mean to study dust extinction and metallicity in the centres of the distant star-forming regions that are almost inaccessible in any other way.

## 2. Spectral change

GRB afterglows typically have featureless piecewise power-law spectra from the X-ray to the optical/near-infrared and radio wavelengths. The simple spectral shape of the GRB spectrum and the lack of X-ray absorption above  $\sim 3$  keV allow us to place constraints not only on the dust reddening but also on the absolute extinction. Theoretically, the most favourable explanation of GRB afterglows is the so-called fireball model (Rees & Mészáros 1992; Mészáros & Rees 1997; Galama et al. 1998b; Sari et al. 1998; Granot & Sari 2002; Zhang et al. 2006). According to the fireball model, GRB afterglows are described by a coherent synchrotron emission from accelerated electrons with a power-law distribution of energies. The afterglow itself is created from synchrotron radiation produced by the interaction between the ultra-relativistic jet and the material in the ISM. At late times, the electron population is expected to radiate in slow cooling regime and the electrons then cool both adiabatically and by emitting synchrotron and inverse Compton radiation. In that regime the GRB spectrum is defined by a broken power-law model producing a cooling break in the synchrotron emission spectrum, which typically located between the X-ray and the

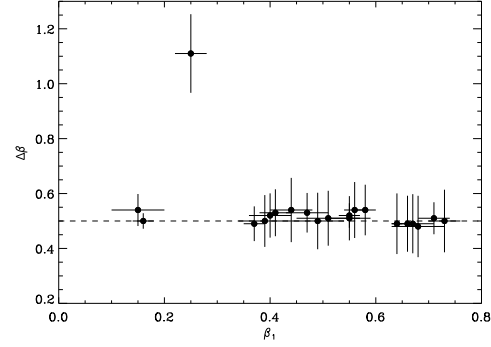


**Fig. 1.** Spectral change,  $\Delta\beta$ , against the optical spectral slope,  $\beta_1$ . GRB 080210 is the only outlier with larger spectral change compared to the rest of the sample.

optical/near-infrared wavelengths. The broken power-law model is given as

$$F_\nu = \begin{cases} F_0 \nu^{-\beta_1} & \nu \leq \nu_{\text{break}} \\ F_0 \nu_{\text{break}}^{\beta_2 - \beta_1} \nu^{-\beta_2} & \nu \geq \nu_{\text{break}} \end{cases} \quad (1)$$

where  $F_0$  is flux normalization,  $\nu$  is frequency and  $\beta_1$  and  $\beta_2$  are spectral slopes of the optical/near-infrared and the X-ray segments respectively.  $\nu_{\text{break}}$  is the cooling break frequency joining the two power-law segments typically between  $10^{14}$  Hz  $\lesssim \nu_{\text{break}} \lesssim 10^{18}$  Hz. Sari et al. (1998) outlined in their theory that in this simple picture this additional break between the X-ray and optical/near-infrared will give a spectral change of  $\Delta\beta = \beta_2 - \beta_1 = 0.5$  resulting in a softer spectrum on the high energy side.

$\Delta\beta$  is treated as a free parameter in the spectroscopic sample study of 41 GRB afterglows by Zafar et al. (2011). Afterglow SEDs of 21 GRBs prefer a break between the X-ray and optical/near-infrared wavelengths. 95% of the spectral breaks have a spectral change consistent with the synchrotron emission model outlined by Sari et al. (1998), i.e.  $\Delta\beta = 0.5$  (Zafar et al. 2011). In Fig. 1 the spectral change is plotted against the optical spectral slope,  $\beta_1$ . The mean spectral change of all 21 GRBs is 0.54 with a standard deviation of 0.13. This large deviation is dominated by only one outlier GRB 080210 having  $\Delta\beta = 1.1 \pm 0.1$ . Excluding outlier, the mean spectral change of

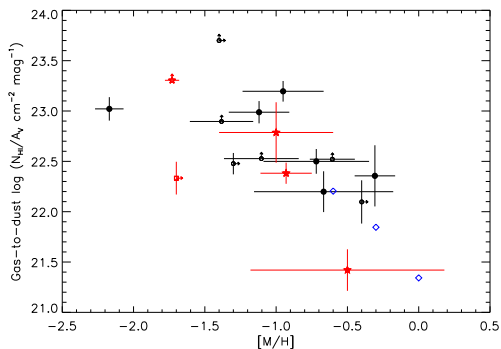


**Fig. 2.** Gas-to-dust ratio against metallicity for GRB afterglows. The Zn based metallicities are marked with red stars. The remaining data points are based on Si based metallicity. GRB 080607 is outside the sample criteria and is indicated with a red square. The gas-to-dust ratios and metallicity upper limits are indicated by small circles or stars. The MW, LMC and SMC environments are denoted with blue diamonds from right to left.

20 GRB afterglows out of 21 is found to be 0.51 with a very small standard deviation of 0.02.

### 3. Gas-to-dust ratios and metallicities

Metallicities measured in GRBs are usually higher than the ones found in damped Ly $\alpha$  absorbers (DLAs) observed through distant QSOs, and vary from less than 1/100 to nearly a solar values (e.g., Fynbo et al. 2006; Prochaska et al. 2007; Fynbo et al. 2008; Ledoux et al. 2009). For a large fraction of GRB afterglows, metallicities are not available either mainly due to the lack of high or medium resolution spectroscopy or a redshift  $\lesssim 2$ , placing the Lyman alpha line outside the observed wavelength range. Metallicities for GRB afterglow sub-sample published in Zafar et al. (2011) are obtained either from literature or using the metallicity–Si II (1526 Å) equivalent width correlation for QSO-DLAs (Prochaska et al. 2008, Eq. 1). The total neutral hydrogen gas column for these GRBs is inferred from the GRB-DLA fitting in Fynbo et al. (2009). Using the dust content from the SED analysis, gas-to-dust ratios are obtained for GRB afterglow sub-sample (see Zafar et al. 2011). In Fig. 2 gas-

to-dust ratios of GRB sub-sample are plotted against the GRB metallicity showing some evidence of an anti-correlation between the two values. The values MW, LMC and SMC environments are also plotted indicating the same trend. A Spearman rank test for a random origin for such an anti-correlation yields a  $< 1\%$  probability. Since dust is composed of metals we expect to see such relation between the two. An anti-correlation between gas-to-dust ratios and metallicities was also previously found for a sample of dwarf galaxies (Lisenfeld & Ferrara 1998) and the *Spitzer* Infrared Nearby Galaxies Survey (SINGS) sample (Draine et al. 2007).

### 4. Comparison with Local Group sightlines

A characteristic feature in the extinction curves of the MW is the 2175 Å extinction bump, first discovered by Stecher (1965). The 2175 Å bump has been attributed to absorption by graphite grains processed by star formation (e.g., Draine 2003). The feature becomes gradually weaker in the LMC and SMC. In Zafar et al. (2011) sample less than 9% of the GRB afterglow extinction curves show an unequivocal 2175 Å bump. Knowing the importance of this feature, the spectroscopic sample of Zafar et al. (2011) is re-fitted with the Fitzpatrick & Massa (1990) dust extinction model. The aim was to get the  $c_3$  parameter of the Fitzpatrick & Massa (1990) dust extinction model which measures the strength of the 2175 Å bump. This was done to see the bump properties and determining the significance of bump for GRB afterglows. We find no significant detection of the strength of the 2175 Å bump for all 38 GRBs with best-fit SMC-type extinction curve in Zafar et al. (2011). We obtained  $2\sigma$  upper limits of  $c_3$  for all these afterglows. To-date the 2175 Å bump is significantly detected in the optical afterglow spectra of four GRB afterglows: GRB 070802, GRB 080605, GRB 080607 and GRB 080805. The results of GRB 070802 and GRB 080607 are used results from the Fitzpatrick & Massa (1990) fitting analysis published in Zafar et al. (2011). The results of GRB 080605 and GRB 080805 are

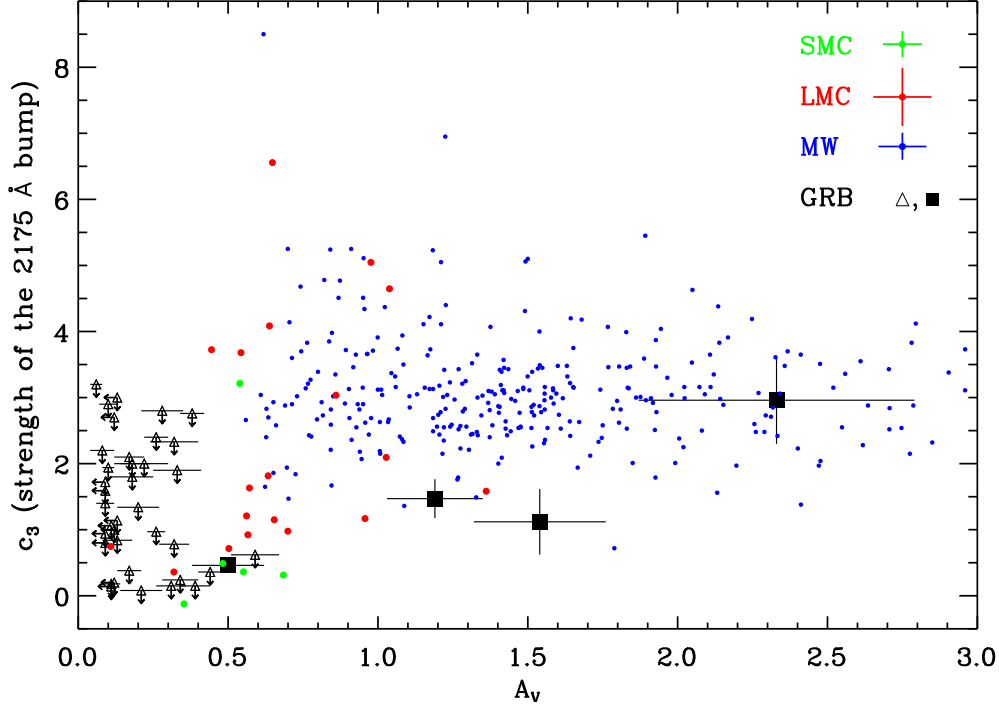


**Fig. 3.** The 2175 Å bump strength,  $c_3$ , versus rest-frame  $V$ -band extinction,  $A_V$ , for spectroscopic GRB sample.  $2\sigma$  upper limits for  $c_3$  and  $A_V$  are denoted by open black triangles. The squares represent the four GRB afterglow cases with the 2175 Å bump detected in afterglow spectra. The blue, red and green circles illustrate lines of sight in the MW, LMC and SMC. The green, red, and blue lines on the top-right corner represent the average errorbar size of the SMC, LMC, and MW data-points respectively.

taken from the analysis performed in Zafar et al. (in prep). In Fig. 3 we plot bump strength,  $c_3$ , of GRB afterglow sample against the  $A_V$  values. We also compared the GRB sample results to the lines of sight in the MW (Fitzpatrick & Massa 2007), LMC and SMC (Gordon et al. 2003). Fig. 3 in fact shows that GRB afterglows usually have small bump strength for a given value of  $A_V$ . The 2175 Å bump strength for a given  $A_V$  is usually lower than the typically observed lines of sight in the Local Group.

## 5. Conclusions

The advantages and possibilities of using GRB afterglows as probes to study gas and dust has been briefly outlined. It has been found that the broken power-law model is consistent with

the simple synchrotron spectrum with a spectral change of half. Like other nearby galaxies, GRBs also indicate an anti-correlation between the gas-to-dust ratios and metallicity. Finally, it has been noted that GRBs usually have smaller value of the 2175 Å bump strength for a given value of  $A_V$ .

*Acknowledgements.* The Dark Cosmology Centre is funded by the Danish National Research Foundation. I am grateful to D. Watson and J. P. U. Fynbo for the helpful discussions.

## References

- Bloom, J. S., Kulkarni, S. R., & Djorgovski, S. G. 2002, *AJ*, 123, 1111  
 Cardelli, J. A., Clayton, G. C., & Mathis, J. S. 1989, *ApJ*, 345, 245

- Draine, B. T. 2003, *ARA&A*, 41, 241  
Draine, B. T., et al. 2007, *ApJ*, 663, 866  
Fitzpatrick, E. L. & Massa, D. 1986, *ApJ*, 307, 286  
Fitzpatrick, E. L. & Massa, D. 1990, *ApJS*, 72, 163  
Fitzpatrick, E. L. & Massa, D. 2007, *ApJ*, 663, 320  
Fynbo, J. P. U., et al. 2009, *ApJS*, 185, 526  
Fynbo, J. P. U., Prochaska, J. X., Sommer-Larsen, J., Dessauges-Zavadsky, M., & Møller, P. 2008, *ApJ*, 683, 321  
Fynbo, J. P. U., et al. 2006, *Nature*, 444, 1047  
Galama, T. J., et al. 1998a, *Nature*, 395, 670  
Galama, T. J., et al. 1998b, *ApJ*, 500, L97  
Gordon, K. D., et al. 2003, *ApJ*, 594, 279  
Granot, J. & Sari, R. 2002, *ApJ*, 568, 820  
Hjorth, J., et al. 2003, *Nature*, 423, 847  
Ledoux, C., et al. 2009, *A&A*, 506, 661  
Lisenfeld, U. & Ferrara, A. 1998, *ApJ*, 496, 145  
Mészáros, P. & Rees, M. J. 1997, *ApJ*, 476, 232  
Pei, Y. C. 1992, *ApJ*, 395, 130  
Prochaska, J. X., Chen, H., Dessauges-Zavadsky, M., & Bloom, J. S. 2007, *ApJ*, 666, 267  
Prochaska, J. X., et al. 2008, *ApJ*, 672, 59  
Rees, M. J. & Mészáros, P. 1992, *MNRAS*, 258, 41P  
Sari, R., Piran, T., & Narayan, R. 1998, *ApJ*, 497, L17  
Stanek, K. Z., et al. 2003, *ApJ*, 591, L17  
Stecher, T. P. 1965, *ApJ*, 142, 1683  
Woosley, S. E. 1993, *ApJ*, 405, 273  
Zafar, T., et al. 2011, *A&A*, 532, A143  
Zhang, B., et al. 2006, *ApJ*, 642, 354